

Polymers for Near-field Electrospinning with Spatial Control

Antonio Osamu Katagiri Tanaka, Héctor Alán Aguirre Soto

Abstract

Near-field electrospinning (NFES) is identified to be a technique able to fabricate polymer nano and micro fibers with accurate placement. In the past years (2006-2019), several polymer solutions have been successfully electrospun into fibers through several variants of the conventional NFES process. Each NFES variant intends to tailor the process parameters in order to improve the fibers' properties. This paper presents a review on the research and related development of electrospun fibers, emphasizing the used polymers, solvents, and fiber characteristics. Relevant summary of polymer solutions and near-field electrospinning processing conditions is provided in this paper.

Keywords: polymer, solvent, near-field electrospinning, NFES, fibers, spatial control

Contents

1 Introduction	2	4.1 Nozzle spinneret	9
1.1 Types of electrospinning (Classified by process properties)	2	4.2 Applied Voltage	10
1.1.1 High voltage power supply: Direct Current & Alternating Current	2	4.3 Nozzle-to-substrate distance	11
1.1.2 Polymer reservoir: Polymer melt & Polymer solution	4	4.4 Electric field	11
1.1.3 Stretching forces	5	4.5 Substrate	12
1.1.4 Dispensing nozzle: Coaxial / Monoaxial: Single nozzle / Multinozzle	7	5 NFES Variants	22
1.1.5 Nozzle-to-substrate distance	7	5.1 Low-Voltage NFES (LV NFES) [8]	22
2 "Electro - DC - monoaxial - solution - NF - spinning"	7	5.2 Scanning Tip Electrospinning [9]	22
3 Polymer Solution	7	5.3 3D Electrospinning [26] Electrohydro-dynamic 3D Print-patterning or Electrohydro-dynamic Jetting [17]	22
3.1 Polymers	8	5.4 Multinozzle NFES [33–35]	22
3.2 Solvents	8	5.5 Electrohydro-dynamic Writing or Mechano-electrospinning (MES) [24] Electrohydro-dynamic Direct-Write (EDW) [37] Mechano-Electrospinning [38]	22
4 Effect of the NFES Parameters	9	5.6 Suspension NFES [39]	22
		5.7 Helix Electrohydro-dynamic Printing (HE-printing) [31] Electrohydro-dynamic (EHD) jet printing [23]	22
		5.8 Airflow-assisted Electrohydro-dynamic Direct-writing (EDW) [32]	22

Email addresses: oskatagiri@gmail.com (Antonio Osamu Katagiri Tanaka), alan.aguirre@tec.mx (Héctor Alán Aguirre Soto)

5.9	Tethered Pyro-Electrohydrodynamic Spinning (TPES) [19] . . .	22
6	Conclusion	22
7	NFES Achievements & Challenges	24
	References	24

1. Introduction

Even though electrospinning is an old invention [1], it is currently a trending topic among researchers [2–4]. One of the reasons electrospinning is to be studied is its potential to fabricate polymer nano-fibers from a variety of polymers. The technique allows the production of thin continuous fibers with ease, with diameters down to 3 nm in some cases, which is something difficult to achieve by other techniques. Furthermore, the basic setup can be modified with ease to fabricate different fibers with diversified functionalities with different materials. The produced fibers can be aligned or unaligned. Besides, the electrospinning equipment is inexpensive and of small size, compared to the equipment of standard spinning techniques [5]. On the other hand, the understanding of the electrospinning process has improved in the last years.

1.1. Types of electrospinning (Classified by process properties)

Current literature dictates the typical spinning setup is comprised by three main components: a syringe needle, a fiber collector, and some way to dispense the fibers from the needle to the collector. The spinning process is an electrohydrodynamic (EHD) technique that yields continuous polymer fibers. Other EHD techniques are spraying and atomization which produce polymer droplets and polymer particles respectively.

In electrospinning the fibers are deposited by an electrical potential difference between the syringe needle and the collector. The supplied polymer (typically a polymer solution) is administrated at a constant rate to create and maintain a polymer drop at the dispensing nozzle. A high voltage (usually DC) is applied between the polymer feed

and the collector. As the electric field increases, the polymer drop (held by its surface tension) is then deformed at the tip of the syringe needle to form a conical shape known as Taylor cone. When the electric force overcomes the surface tension force a polymer jet is ejected from the tip of the Taylor cone. As the polymer jet leaves the nozzle, it accelerates and stretches while traveling to the fiber collector. The fiber finally develops with the complete solvent evaporation.

1.1.1. High voltage power supply: Direct Current & Alternating Current

Electricity comprises a flow of electrons (negatively charged subatomic particles). In direct current (DC; used for the vast majority of electrospinning work) the electrons flow in one direction continually. It is also possible to have alternating current (AC), which is used to power most electrical devices in the home. AC involves a periodic change in the direction of current flow: that is, the electrons first flow in one direction and then switch to flow in the reverse direction. The switch between directions is repeated many times per second and is known as the frequency of the AC. Using an AC power supply rather than the conventional DC supply was first shown to generate polymer-based nanofibres in 2004. [3]

The experimental set-up for AC electrospinning is similar to that for the DC process, but it does not require a grounded collector. Because the current alternates, the fibres produced at one instant in time carry a positive charge, while those generated shortly thereafter have a negative charge. The positive and negative fibres thus discharge on each other, which results in an aerogel plume of fibres. The frequency of the AC current determines whether charge carriers of one polarity have sufficient time to charge the solution and result in spinning. The optimal AC frequency is material-dependent and typically in the range of 50 Hz–1 kHz. [4]

The AC approach has been explored for the fabrication of drug-loaded fibres in a few recent studies. In one, Balogh et al. undertook a direct comparison of fibres prepared by DC and AC spinning. They used the beta-blocker carvedilol as a

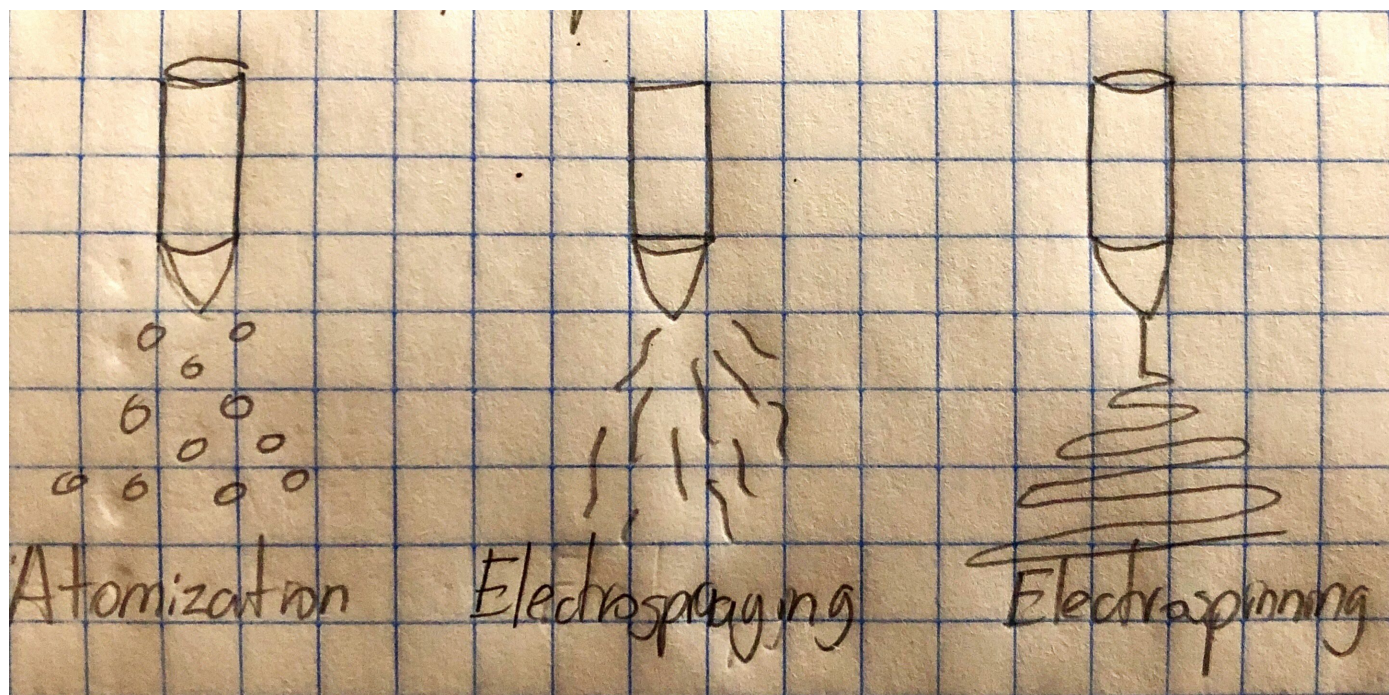


Figure 1: Electrohydro-dynamic techniques

model drug, and fibres were generated using three different polymers: Eudragit EPO, a cationic copolymer soluble below pH 5.0; Eudragit L100-55, an anionic polymer soluble above pH 5.5; and the neutral polymer poly(vinyl pyrrolidone) (PVP). It was found that fibres could be generated with all three polymers from both types of spinning, but that it was possible to use much faster flow rates in the AC process. With DC spinning, a maximum flow rate of 5 ml h⁻¹ could be achieved, whereas with AC this could be increased to up to 40 ml h⁻¹. All fibres, from both processes and made from all polymers, existed as amorphous solid dispersions. The drug release profiles were studied, and the AC and DC fibres were found to be indistinguishable in their performance. [Adapted with permission from Balogh, A.; Cselko, R.; Demuth, B.; Verreck, G.; Mensch, J.; Marosi, G.; Nagy, Z. K. 'Alternating current-electrospinning for preparation of fibrous drug delivery systems.' *Int. J. Pharm.* 495 (2015): 75–80. Copyright Elsevier 2015.]

The same team have also compared AC and DC electrospinning of blends of hydroxypropylmethylcellulose (HPMC) and poly(ethyleneoxide) (PEO) with the poorly water-soluble diuretic spirono-

lactone. [6] Both HPMC and PEO alone could be processed by the DC approach. In contrast, AC electrospinning of HPMC led to a mixture of droplets and fibres, and high-molecular-weight PEOs did not yield any solid products at all in the AC method. Selecting appropriate blends of the two polymers, however, permitted high-quality fibres to be formed via AC spinning.

AC processing of HPMC or PEO with spironolactone also proved to be problematic, but again with the right mix of HPMC and PEO drug-loaded fibres could be generated. These were able to accelerate the dissolution rate of the drug, even at loadings of up to 40% w/w. The AC-generated fibres were found to be several orders of magnitude thinner than the DC electrospun fibres despite the flow rate being three times faster in the AC process.

Similar observations have been reported using HPMC acetate succinate (HPMCAS) and spironolactone. [7] HPMCAS could not be processed by either DC or AC electrospinning; the addition of PEO permitted fibres to be produced with the DC approach, but not using AC, and the addition of an ionic surfactant or salt was required to produce high-quality fibres with AC spinning.

As with HPMC, the HPMCAS fibres led to a significant enhancement in the dissolution rate

It is thus clear that AC electrospinning is similarly effective to the DC approach in producing drug delivery systems. Although its use in this regard is in its infancy, given the fact it allows higher throughput than the DC technique, it seems certain that this is an approach which is likely to receive much more attention in the coming years.

1.1.2. Polymer reservoir: Polymer melt & Polymer solution

Another variant of electrospinning which has attracted some attention in the drug delivery sphere is the melt process. This is discussed in detail in a recent review. [8] In brief, the process is analogous to the solution electrospinning discussed in previous sections, but in place of a polymer solution a melt is used. This adds some complexity to the process, because the syringe and spinneret must be heated to maintain the polymer in its liquid state. Further, the elevated temperature can potentially lead to drug degradation, since many drugs are thermally labile. The fibres produced in melt spinning are typically found to have larger diameters than those from the solution route due to the significantly higher viscosity of a polymer melt than its solution form. The apparatus used is depicted in [TODO: draw an apparatus used for melt electrospinning].

Despite these apparent disadvantages, there are a number of attractive aspects of the melt spinning process, not least the fact that it obviates the need to handle large volumes of volatile solvents. This both renders the process safer, particularly if it is to be performed on the larger scale, and precludes any solvent contamination in the products.

The first report of a melt electrospun drug delivery system came from Nagy and co-workers, who prepared melt-spun fibres of Eudragit EPO loaded with carvedilol. [9] The drug and polymer were melted and mixed to form a homogeneous solid mixture prior to spinning, and then processed as in a solution experiment but with both the syringe and spinneret heated. The melt fibres were much wider than analogous system-

processed through solution spinning, with those from melt processing having diameters of 5–30 μm , as compared to 300–1000 nm for the solution-spun fibres. The drug was completely amorphously dispersed in the fibers regardless of the processing route. This is as expected for solution spinning, and in the melt case was thought to be because the experiment was carried out above the melting point of carvedilol. The melt fibres freed their drug loading faster than the solution-spun analogues, despite the much larger surface area of the latter. The authors ascribed this to the fact that the melt fibres had a loose nonwoven structure, whereas those prepared by solution spinning were more tightly packed.

This work has been built on to blend plasticisers with the polymer Eudragit E and carvedilol active ingredient. [10] The plasticisers triacetin, Tween 80 and polyethylene glycol were all investigated with the goal of reducing the melting point of the polymer/drug blend and thereby permitting lower temperatures to be used for spinning. This should reduce the likelihood of any degradation occurring. High-performance liquid chromatography data obtained on dissolved fibres revealed that the addition of plasticisers clearly reduced the amounts of carvedilol degradation products present after melt spinning

A direct comparison of poly(ϵ -caprolactone) (PCL) fibres generated by the melt and solution-spinning approaches has been reported by Lian and Meng. [11] These authors prepared curcumin-loaded fibres of around 4 μm in diameter using both techniques. They found that there was a greater tendency for the curcumin to crystallise using the solution route (a result of its low solubility in the solvent used for spinning). The melt fibres led to a reduced burst release and a slower release rate. These findings were attributed to the solution-spun fibres having a porous structure, which permitted both water ingress and the incorporated curcumin to diffuse out of the polymer matrix

Melt electrospinning typically generates micron-size fibres. In a recent effort, however, highly uniform and precise deposition of PCL nanofibres (817 ± 165 nm) was achieved us-

ing a method known as melt electrospinning writing. [12] This combines melt electrospinning with additive manufacturing (three-dimensional (3D) printing) technology, using a computer-controlled extruder moving on a translational stage to build a 3D structure layer by layer. The 3D fibrous architecture produced allowed efficient in vitro proliferation of primary human mesenchymal stromal cells. The melt electrospinning writing technology can produce regular 3D morphologies in a highly controllable and reproducible fashion, and is currently being explored for a range of tissue-engineering applications.

Although melt electrospinning has received much less research interest than the solution process, it appears to be equally as flexible in terms of handling multiple fluids, and coaxial melt spinning has been reported. [13] The initial melt spinning experiment is perhaps harder to establish than the solution route, but it is clear that this approach has a great deal of unexplored potential in the development of drug delivery systems.

1.1.3. Stretching forces

Centrifugal force. Centrifugal spinning employs a rotating polymer source to generate fibres. Several centrifugal methods can generate nanofibres. These include Forcespinning, which employs rotary speed of above 2000 revolutions per minute (rpm), [14] electrocentrifugal spinning, [15] which combines a strong electric potential (as in electrospinning) with centrifugal force, and pressurised gyration, which adds high pressure (> 10 kPa) to centrifugal spinning to enhance fibre formation (see section 6.8). [16]

These approaches can be applied to polymer solutions and emulsions, and if the source can be heated also to a polymer melt [TODO: draw an apparatus used for centrifugal spinning]. [17] This technique has received some attention in the context of drug delivery. For instance, Zander prepared PCL fibres using both the solution and melt variants of the centrifugal technique. [18] This author employed spinning speeds in the range of 3000–18,000 rpm, yielding fibres of $10\text{ }\mu\text{m}$ in diameter. PC12 neuron cells could be successfully grown on the fibres, demonstrating that they have

potential in nerve tissue engineering.

In other work, centrifugally spun PCL/PVP fibres containing the antibiotic tetracycline have been produced from a methanol/chloroform solution at 2000 rpm. [19] These were sub-micron in their diameters, and highly aligned. The rate of drug release could be tuned by varying the PCL/PVP ratio in the fibres, and the fibres were found to be effective in inhibiting bacterial growth. Core/shell fibres for the delivery of growth factors have further been reported from centrifugal spinning of a water-in-oil emulsion, with PCL dissolved in the oil phase. [20]

Fibres have also been made using a melt process with sucrose (a sugar dimer) loaded with a range of poorly water-soluble drugs, including olanzapine (an antipsychotic medicine) and piroxicam (a non-steroidal anti-inflammatory). [21] The fibres were $10\text{--}15\text{ }\mu\text{m}$ in diameter, and the dissolution rate of the drugs enhanced after fibre formation.

Since the centrifugal spinning approach is a simple one which allows relatively large-scale production of fibres, [22] it appears to have much promise in the drug delivery field. It can also be coupled to electrospinning, with both centrifugal and electrical forces applied simultaneously to drive solvent evaporation. [15] Such centrifugal-electrospinning uses the same equipment as the standard centrifugal process but additionally applies a high voltage between the rotating spinneret and the collector. It has been reported to lead to significantly higher throughput than standard electrospinning, [23] and to produce highly aligned fibres. [23, 24] Centrifugal electrospinning has further been demonstrated to have potential in the production of drug delivery systems, with a recent report of PVP fibres loaded with the antibiotic tetracycline hydrochloride. [25] Production rates of up to 120 g h^{-1} could be realised.

Blowing forces. A pressurised gas can be exploited to produce nanoscale fibres, starting either with a polymer solution in a technique known as solution blowing or from a molten polymer source (melt blowing). The experimental apparatus used is similar to electrospinning, in that a polymer solution (or melt) is expelled through a needle (spin-

neret) at a controlled rate. The spinneret is surrounded by an outer nozzle which applies pressurised gas to the fluid being expelled, as illustrated in [Figure apparatus used for solution blow spinning or melt blowing]. [26]

A few studies have explored solution blowing in drug delivery, with the first such work being from Oliveira et al. in 2013. [27] These authors prepared poly(lactic acid) (PLA) fibres loaded with the hormone progesterone, which can be used to regulate the reproductive cycle in livestock. Fibres were produced from solutions with 6% w/v PLA and between 0 and 8% w/v progesterone. The PLA is semi-crystalline both before and after processing, while the drug is amorphous post-spinning. The fibres behave very similarly in terms of their release behaviour, regardless of the amount of drug loaded.

A study comparing electrospun and solution-blown fibres of poly(3-hydroxybutyrate-co-3-hydroxyvalerate) loaded with sodium diclofenac has also been reported. [26] The drug-loaded fibres were slightly larger in diameter when generated by electrospinning, and the size uniformity was higher through solution blowing. In general there was a greater amount of burst release seen with the electrospun fibres, but otherwise there were no clear trends in the drug release data.

Solution-blown fibres have additionally been created loaded with oil extracted from the medicinal plant *Copaifera* sp., which is often explored for antimicrobial purposes. [28] These materials were constructed from a blend of the polymers PLA and PVP, and were around 1 μm in diameter. An increased PVP content was found to result in increased antibacterial activity after 24 h.

The melt blowing process has also received some attention in the pharmaceutical setting, and the fibres produced compared with those from both solution and melt electrospinning. [29] Marosi's team generated formulations from a vinylpyrrolidone–vinyl acetate copolymer, employing poly(ethylene glycol) (PEG) as a plasticiser and carvedilol as a model drug. All three methods led to fibres, with the solution electrospun fibres narrowest (at 2 μm in diameter), followed by the melt-blown (10 μm) and melt-spun

(50 μm) products. Carvedilol was rendered into the amorphous physical form by all three processing techniques, and all the formulations were able to accelerate the drug dissolution process. The melt-blown and melt electrospun systems led to the fastest release, with almost identical release profiles, while the solution-electrospun fibres freed their drug cargo somewhat more slowly.

A variant of the solution-blowing technique has been applied to the processing of living cells (in this setting it has been referred to as *biothreading*). [30] Using a pressurised coaxial needle with the exterior fluid comprising a viscous polydimethylsiloxane solution and an aqueous cell suspension in the core, cells can be processed into scaffolds with nonnoticeable loss in viability.

Electrospinning and melt/solution blowing can be combined in a process known as *electroblowing*. This employs both electricity and a gas flow to aid fibre elongation and solidification. The experimental apparatus uses a similar spinneret to that in [Figure apparatus used for solution blow spinning or melt blowing], and in addition to the gas flow a potential difference is applied between the spinneret and the collector. This technique has been shown to have significant potential in medical applications: in 2014, Jiang et al. applied electroblowing *in vitro* and *in vivo* to deliver a homogeneous and continuous layer of a medical glue to stop bleeding during liver resection. [31]

More recently, Balogh et al. prepared fibres of 2-hydroxypropyl- β -cyclodextrin loaded with sodium diclofenac. [32] They found that when electrospinning this system, very frequent clogging of the spinneret occurred. Electroblowing overcame this issue and additionally allowed faster flow rates to be used, increasing the amount of material that could be produced. However, the uniformity of the fibre products was compromised, with more 'beads-on-string' type morphology seen with the blown products. In both cases, the fibres comprised amorphous solid dispersions with no crystalline drug evident. The electroblown fibres dissolved a little more slowly than those from electrospinning, but still much more rapidly than a physical mixture of drug and cyclodextrin.

A subsequent study using Eudragit E and itra-

conazole (an antifungal active pharmaceutical ingredient) also found that a faster flow rate could be used in blowing, but that the fibre products from the latter had less regular morphologies. [33] Again, the drug was amorphously dispersed in the fibres, and the dissolution profiles of the electrospun and electroblown systems were very similar.

Electric force.

Microfluidic forces. Microfluidic spinning is based on the use of micro (sub-millimetre) channels. A large number of these are located in a single microfluidic chip, and the rate and time of liquid expulsion from each channel are precisely controlled by computer. Microfluidic spinning can be coupled with electrospinning, as described in detail in a recent review by Cheng et al. [51] While the productivity of microfluidic methods is a major challenge in scale-up, the technique offers the ability to generate fibres with a high level of complexity not easily achievable by electrospinning. For example, using a digitally programmed microfluidic flow, Kang et al. created functional microfibres with continuous spatiotemporal coding along the length of the fibre. [52] The fibres contained varied chemical compositions and topography, and localised bioactive agents.

Microfluidic spinning therefore has the potential to enable very precisely tuneable loading of different drugs into a single fibre, allowing for programmable release in different parts of the body at different times. The technique is beginning to be explored for drug delivery applications. However, the materials used in microfluidics are usually hydrogels (crosslinked polymer networks solvated with water). These often have fast degradation rates and as a result can be unsuitable for the extended release of drugs, particularly small molecules. To help mitigate this problem, Chae et al. developed a microfluidic spinning method using an isopropyl alcohol sheath flow with an aqueous alginate core flow. [53] This innovation resulted in nanofibres made of highly ordered alginate molecules. Ahn et al. loaded ampicillin into alginate fibres prepared in this manner, [54] and found that the ordered structure delayed

fibre degradation, allowing extended-release profile of ampicillin over 7 days.

Mechanical force.

1.1.4. Dispensing nozzle: Coaxial / Monoaxial: Single nozzle / Multinozzle

1.1.5. Nozzle-to-substrate distance

Near Field Spinning. Figure 2 describes a typical near-field electrospinning set-up [5]. Two sub-techniques can be derived from electrospinning depending on the distance between the dispensing electrode and the collector. The process in which the electrospun jet can be controlled near the tip is called NFES or near-field electrospinning [6]. Moreover, if the distance between the collector and the dispensing needle is greater, the configuration is known as FFES or far-field electrospinning [7].

Far Field Spinning. In a far field electrospinning the process continues ... Decreasing the jet diameter, the surface charge density increases and the resulting high repulsive forces split the jet into several smaller jets. The jet is seriously elongated by a bending and whipping processes caused by electrostatic repulsion initiated at small bends in the fiber, until it is finally deposited on the collector. Two types of collector may be used, either stationary or rotary collector.

2. "Electro - DC - monoaxial - solution - NF - spinning"

Near-field electrospinning is considered to be an outstanding technique to fabricate polymer fibers with spatial control and it has suffered several modifications to improve the precision and accuracy of the fiber deposition. This paper intends to collect the NFES variants of electrospun polymer solutions with spatial control in recent research.

3. Polymer Solution

In electrospinning, it is typically agreed that the diameter of the fibers increased with higher

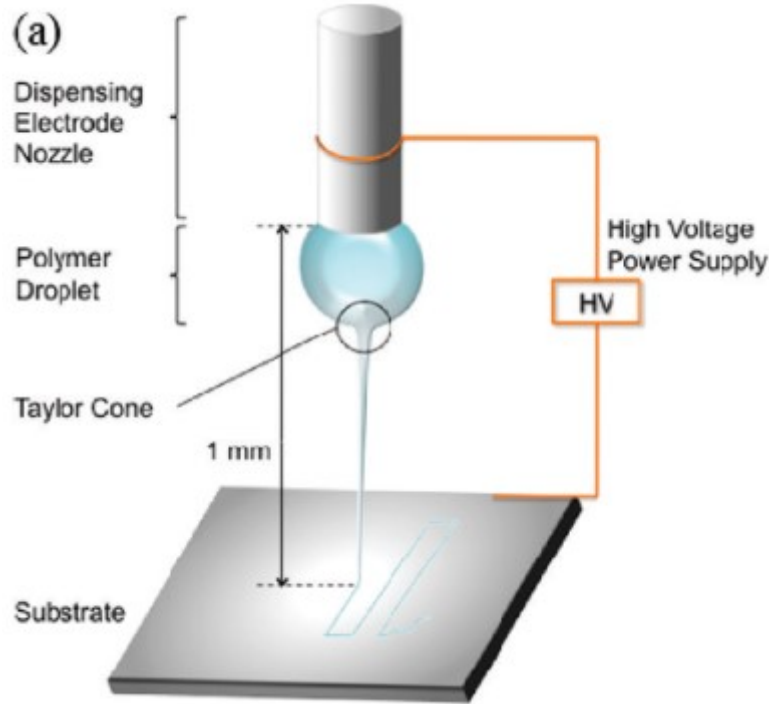


Figure 2: Typical near-field electrospinning set-up [8] .

concentration due to greater viscosity which withstands stretching. In near field electrospinning, similar observations have been reported where concentration increases, fiber diameter increased [9, 10]. However, in separate studies by Pan et al. [11, 12] using poly(γ -benzyl α , l-glutamate) and polyvinylidene fluoride (PVDF) reported reduction in fiber diameter with increasing concentration.

3.1. Polymers

The polymer selection is in function on the intended application. For example, a fast dissolving hydrophilic polymer such as poly(ethylene oxide) (PEO) is used for fast drug delivery systems. Otherwise, slow dissolving polymers such as poly(ϵ -caprolactone) (PCL) or poly(lactic-co-glycolic acid) (PLGA) are implemented. [13]

The polymer molecular weight along with the polymer concentration and solvent selection have a direct effect on the solution viscosity, conductivity and surface tension, hence the solution behavior in the electrospinning process. The spunable viscosity range varies with the polymer and solvent.

Solutions with low viscosity are prone to insufficient polymer chain entanglements to produce fibers. [13] On the other hand, if the solution is too viscous, then the surface tension cannot easily be overcome by the electric field. In both cases, the result can be droplets or particles forming rather than fibers; see Table 1.

3.2. Solvents

The solvent used must be capable of dissolving the polymer of interest at an appropriate concentration to form fibers, and must possess a suitable volatility. A low-volatility solvent like water may fail to evaporate completely over the distance between the spinneret and the collector. When the fibers form, they will hence contain residual water owing to this incomplete evaporation. The residue solvent will subsequently evaporate from the fibers upon storage, resulting in ribbon-like (flattened) fibers, wrinkles on the fiber surface or fused fibers. On the other hand, a high-volatility solvent may evaporate very quickly, leading to larger fiber diameters (less time for elongation before solidification) and clogging of the spinneret (due to drying of the liquid at the spinneret before

Table 1: Approximation process to estimate the critical polymer concentration. Several polymer concentrations are tried and the resulting jets are observed until a continuous stream is achieved.

Observation	Concentration Adjustment
Dripping, no stream	Increase
Splitting small droplets	Increase slightly
Steady stream	No concentration adjustment
Splitting large globs	Decrease slightly
Nozzle clogging	Decrease

jetting, or drying of the Taylor cone during jetting). Solvents commonly used for electrospinning include ethanol, chloroform, dichloromethane and hexafluoroisopropanol.

Mixtures of miscible solvents can be used to ensure that sufficient polymer can be dissolved to give a solution of appropriate viscosity and volatility with suitable dielectric constant range to allow fiber formation. However, care must be taken because using a mixture of solvents with very different volatilities can result in porous fiber structures, as reported by Katsogiannis et al. for organic solvent mixtures with dimethyl sulfoxide (DMSO). [14] DMSO evaporates much more slowly than the organic solvents used, which results in its incorporation into the fibers. The DMSO will eventually evaporate, yielding porous fibers.

It is also important to take into account the surface tension of the solution. Solvents with very high surface tensions (e.g. water) can result in instability arising during the spinning process, and a broad range of fiber diameters in the products. If necessary, a surfactant can be added to reduce the surface tension, but this will be incorporated into the fibers produced.

4. Effect of the NFES Parameters

To spin nano fibers at close distances, the initial diameter of the jet is required to be as small as possible since stretching of the thread is limited. Kameoka et al. [15] demonstrated that a small initial spinning radius can be achieved using an atomic force microscope tip with a small polymer solution drop at the tip.

Near-field electrospinning, has exhibited to be capable fabricate nano fibers over and nano fiber patterns [16]. Nevertheless, having a small polymer solution drop at the nozzle tip limits the length of the fibers that can be fabricated in a continuous manner. Using a spinneret with a reservoir (e.g. syringe) of solution generally produces fibers with diameter of a few micrometers [17, 18], since it creates a limit to which the nozzle inner diameter can be reduced to allow the solution to flow through.

Coppola et al. [19] have showed a NFES variant that allows polymer nano fibers to be deposited directly from a polymer drop, averting the issue of nozzle clogging. The fibers are also prone soaking after deposition thus giving the fibers a semi-circular cross-section as depicted in Xue et al.'s [18] work.

4.1. Nozzle spinneret

The thinnest nozzles in literature so far are about 100 μm in diameter, for instance Chang et al. [9] used a 100 μm inner diameter needle tip to electrospin poly(ethylene oxide) (PEO) and Camillo et al. [20] used a micro-diameter tip Tungsten spinneret in a 26G needle to electrospin co-polymer, poly[2-methoxy-5-(2-ethylhexyloxy)-1,4-phenylenevinylene] (MEH-PPV) with poly(ethylene oxide) (PEO). The nozzle most commonly comprises a simple narrow-bore, blunt-end metal needle. The diameter of the needle can vary, but most commonly researches work with internal diameters below 1 mm . This translates to needles of gauge 18–22. In general, this simple spinneret design can be used to achieve successful spinning. A blunt-

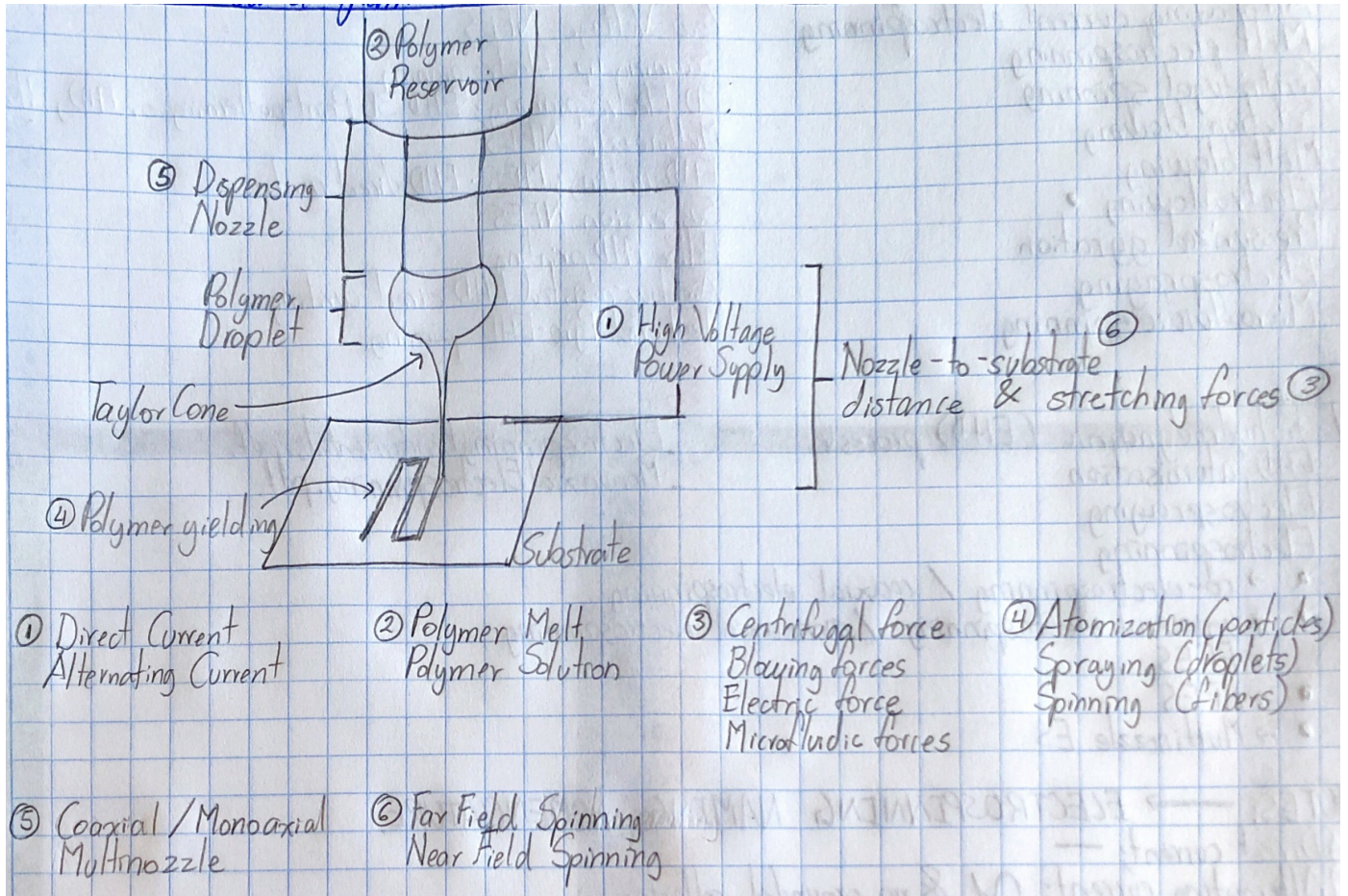


Figure 3: Near-Field ES Process Parameters

end rather than a tapered-end for the needle exit is important as the size distribution of the products increase with an increase in needle tip angle. However, it should be noted that there will be some interactions between the solvent and polymer molecules in the solution and the metal surface of the spinneret. There will exist some attractive forces between the polar groups in the polymer and the electropositive metal surface, which can act counter to the drawing force of the electric field and can pull the polymer solution back into the spinneret. It has been found that coating the spinneret exterior in a non-conductive and non-stick polymer such as Teflon can reduce these interactions. [21] As a result, the electrical energy can be more efficiently used to elongate and narrow the polymer jet, and narrower fibers can be produced. In addition, strong attractive forces between the polymer jet and the metal spinneret can result in fibers becoming attracted

to the needle, leading to lower yields and potentially to blocking of the exit orifice. This effect too can be ameliorated using an epoxy coating. [22]

4.2. Applied Voltage

In recent literature, near field electrospinning has been studied to reduce the fiber diameter and to improve the fiber deposition accuracy. Camillo et al. [20] demonstrated that the application of a modified fine tip nozzle enables the fabrication of 100 nm diameter fiber at a nozzle-to-substrate distance of 500 μm and an applied voltage of 1.5 kV. On the other hand, Bisht et al. [8] and Chang et al. [9] came to the conclusion higher voltages yield thicker micro-fibers with a loss in jet stability.

This discrepancy in literature between the applied voltage and resulting fiber diameter is due to the relationship with other variables such as

nozzle-to-substrate distance and solution deposition rate. For instance, if a high voltage is applied at a low deposition rate then electrospraying is achieved, meaning the formation of several non-continuous fibers. The applied voltage shall be sufficient to break the surface tension and initiate the jet, but low enough to avoid multiple jets at the nozzle tip.

Bisht et al. [8] achieved the fabrication of thinner fibers with spatial control by reducing the applied voltage to 200-600 V at a nozzle-to-substrate distance of 0.5-1 mm. The low voltage setting does not create enough charge to break the polymer solution surface tension to initiate the electrospinning process.

Bisht et al. [8] and Chang et al. [9] initiated the electrospun fibers by mechanically pull the polymer solution at the nozzle tip using a micro-probe tip. Chang and coworkers reduced the applied voltage from 1.5 kV to 600 V with a nozzle-to-substrate distance of 500 μm to yield a fiber diameter between 3 μm and 50 nm. With an applied voltage of 200 V and a nozzle-to-substrate distance of 1 mm, PEO nano fibers were deposited with a diameter about 20 nm.

In near-field electrospraying, the applied voltage has an impact on the produced fiber morphology. For instance, a voltage higher or lower to the optimum voltage will translate into an increase in fiber diameter. Song et al. [23] demonstrated that a decrease in voltage from 400 to 500 V can reduce the fiber diameter from 160 to about 60 nm with a nozzle-to-substrate distance of 20 μm . The optimum voltage is achieved when a balance is attained between the stretching of the jet and the speed at which it hits the substrate. The increase of voltage yields thinner fibers as it causes greater stretching, and a greater jet acceleration.

Another workaround to break the polymer solution surface tension is to initialize the NFES process with a higher voltage and then lower the voltage once the jet is created. Huang et al. [24] implemented the previous and yield ordered fibers with a distance between adjacent fibers of 50 μm . In most cases, a positive voltage is applied to the spinneret.

4.3. Nozzle-to-substrate distance

In NFES, the fiber morphology can be altered by the control of the height between the nozzle and the substrate (collector). With the decrease of the nozzle-to-substrate distance, the electric field strength increases; however it can cause incomplete solvent volatilisation and possible short circuits between the collector and the nozzle tip.

An optimal nozzle-to-substrate distance shall be defined to ensure the fabrication of dry continuous fibers. If the solvent is not well evaporated, the produced fibers are prone to defects; on the other hand if solidification happens too fast, the solids can block the spinneret which can prevent a continuous fiber yield. Furthermore, the polymer jet will discharge itself as soon as possible, therefore long distances can result in low yields.

Typically, metal nozzle tips are used, with small inner diameters. From literature, needles with small diameters produce thinner fibers. A thin nozzle tip can help the reduction of the fiber diameter, but also it is more likely to become blocked.

4.4. Electric field

Recent literature suggests that the fiber morphology depends on the electric field profile created by the applied voltage during NFES. Since the electric field is an induced force that attracts the solution jet towards the desired location within the collector.

Bisht et al. [8] and Min et al. [25] have reported the ability to electrospin nano fibers with high accuracy. Min et al. [25] implemented a NFES setup with multiple "field-effect transistors" on a flexible polyacrylate collector with an x-y stage velocity of 13.3 cm/s to fabricate fibers with a diameter about 289 nm and a distance between adjacent fibers of 50 μm .

On the other hand, Bisht et al. [8] showed evidence of fabricated fibers with low-voltage NFES with high accuracy and precision. Bisht et al.'s suspended fibers were deposited over carbon posts with a distance between adjacent fibers of 100 μm with diameter of 30 μm [8].

The employment of guided electrodes in NFES, adapts the fabrication process to yield a more accurate fiber deposition. For instance, Kim et

al. [26] manufactured ink patterns on a paper with silver nano particles. The printed patterns aid the fibers to land on the desired location. Kim et al. [26] electrospun the fibers with a distance between adjacent fibers of $150\ \mu m$.

Xu et al. [27] created a straight jet from the nozzle tip to the substrate using a guiding electrode underneath the collector. The purpose of the guiding electrode is to adjust the path of the NFES jet. With the guiding electrode implementation, the fiber's spread was reduced from $74\ \mu m$ to $7\ \mu m$.

4.5. Substrate

Due to the close distance between the grounded substrate and the charged spinneret in NFES, the set up is prone to electrical shorts. In NFES, when a short circuit takes place, the electrospinning process is interrupted resulting in the fabrication of discontinuous fibers. Two workarounds to avoid electrical shorts is to lower the applied voltage and to install less conductive substrates [28, 29].

Liu et al. [28] discovered that the fiber alignment is improved by using a glass-cooper foil substrate, however the well aligned fibers are spoiled after prolonged depositions due to residual charges. Additionally, the effect of residual charges is amplified with the used collector substrate contains a conductive layer and a non-conductive layer [28].

On the other hand, Choi et al. [29] implemented a hydrophobic substrate to deposit the fibers with plasma treatment to increase the conductivity of selected areas. NFES was carried out with precise deposition as the fibers were placed as per the desired design within the hydrophilic substrate.

Table 2: Electrospun Polymer Solutions - Solution and Process Parameters

Polymer(s)	Solvent(s)	NFES Variant	Process Parameters and Fiber Characterization	Ref.
Poly(ethylene oxide) (PEO; MW = 4,000,000 <i>g/mol</i>)	Deionized water	Low-Voltage NFES (LV NFES)	Solution Concentration: 1, 2, and 3 <i>wt%</i> PEO Nozzle: 27 gauge type 304; stainless steel needle Solution deposition rate: lower than 1 μ L/h Nozzle-to-substrate distance: 1mm Substrate composition: Pyrolyzed SU-8 carbon and Si Applied voltage: polymer jet initiated at 400-600 <i>V</i> and dispensed at 200-400 <i>V</i> x-y stage velocity: 10-40mm/s Fiber Diameter: 50-425nm Distance between adjacent fibers: <i>Not determined</i>	[8]
13 Poly[2-methoxy-5-(2-ethylhexyloxy)-1,4-phenylenevinylene] (MEH-PPV; MW = 380,000 <i>g/mol</i>) with Poly(ethylene oxide) (PEO; MW = 300,000 <i>g/mol</i>)	acetonitrile toluene mixture (65/35); acetic acid toluene (17/83); pure toluene	Typical NFES process	Solution Concentration: 10mg of MEH-PPV in 2mL of toluene; 500 μ L of MEH-PPV solution with 250mg of PEO in 3.5mL of acetonitrile / toluene (65 / 35); 500 μ L of MEH-PPV solution with 250mg of PEO in 3mL of acetic acid / toluene (17 / 83). The resulting MEH-PPV/PEO concentration is 0.08 <i>wt%</i> Nozzle: mm-diameter tip Tungsten spinneret in a 26 gauge needle Solution deposition rate: 50 μ L/h Nozzle-to-substrate distance: 500 μ m Substrate composition: SiO ₂ /Si (oxide thickness = 800 nm) Applied voltage: around 1.3kV x-y stage velocity: 50cm/s Fiber Diameter: 100nm Distance between adjacent fibers: around 100 μ m	[30]

Continued on next page

<i>Table 2 continued</i>				
Poly(ethylene oxide) (PEO; MW = 300,000 g/mol)	Water	Scanning Tip Electrospinning and NFES	<p>Solution Concentration: 7wt% PEO [9]</p> <p>Nozzle: Needle outer diameter of 200μm and inner diameter of 100μm</p> <p>Solution deposition rate: 0.1μL/h</p> <p>Nozzle-to-substrate distance: 500μm</p> <p>Substrate composition: <i>Not determined</i></p> <p>Applied voltage: polymer jet initiated at 1.5 kV and dispensed at 600V</p> <p>x-y stage velocity: 120mm/s</p> <p>Fiber Diameter: 709\pm131nm; 49-74nm when applied voltage is 800V</p> <p>Distance between adjacent fibers: <i>Not determined</i></p> <p>Notes: 108m yield in 15min with a fiber diameter of 709\pm131nm</p>	
Poly(vinylidene fluoride) (PVDF; MW = 440,000 g/mol)	N,N Dimethylformamide (DMF)	Helix Electrohydrodynamic Printing (HE-printing)	<p>Solution Concentration: 1.8g PVDF in 4.1g of DMF and 4.1g of acetone. The resulting concentration is 18% PVDF. [31]</p> <p>Nozzle: Needle outer diameter of 510μm and inner diameter of 260μm</p> <p>Solution deposition rate: 400nL/min</p> <p>Nozzle-to-substrate distance: 10-50mm</p> <p>Substrate composition: Poly(dimethylsiloxane) (PDMS) on Ecoflex</p> <p>Applied voltage: 1.5-3kV</p> <p>x-y stage velocity: 0-400mm/min</p> <p>Fiber Diameter: about 1.5-3μm</p> <p>Distance between adjacent fibers: <i>Not determined</i></p>	

Continued on next page

Table 2 continued

15	Polyhedral Oligomeric Silsesquioxane-Poly(Carbonate-Urea)Urethane (POSS-PCU) and Polyhedral Oligomeric Silsesquioxane-Poly(Caprolactone-Poly(Carbonate-Urea)Urethane) (POSS-PCL-PCU) (Dry Polycarbonate MW = 2000 g/mol)	Dimethyl acetamide (DMAC) and 1-Butanol	Electrohydrodynamic 3D Printing or Electrohydrodynamic Jetting	Solution Concentration: POSS-PCU and POSS-PCL-PCU used in 20%w/w concentration in DMAC Nozzle: needle of 750 μm in diameter Solution deposition rate: less than 1 $\mu L/min$ Nozzle-to-substrate distance: about between 500 μm to 2mm Substrate composition: Not determined Applied voltage: 8.0-10.0kV x-y stage velocity: 10mm/s Fiber Diameter: 5-50 μm Distance between adjacent fibers: 250 μm	[17]
	Poly(ethylene oxide) (PEO; MW = 300,000 g/mol)	Distilled water	Electrohydrodynamic Writing or Mechano-electrospinning (MES)	Solution Concentration: 6wt% PEO Nozzle: Not determined Solution deposition rate: 1200nL/min Nozzle-to-substrate distance: 7.5mm Substrate composition: Not determined Applied voltage: polymer jet initiated at 2 kV and dispensed at 0.8-1kV x-y stage velocity: around 400mm/s Fiber Diameter: 200-350nm Distance between adjacent fibers: 5 μm	[24]

Continued on next page

Table 2 continued

Poly(ethylene oxide) (PEO; MW = 300,000 g/mol)	Deionized water and ethanol with a volume ratio of 3:1	Airflow-assisted Electrohydrodynamic Direct-writing (EDW)	Solution Concentration: 8wt% PEO [32] Nozzle: Outer airflow passage diameter: 1mm Airflow gas pump pressure: 25kPa Inner liquid passage diameter: 0.21mm Solution deposition rate: 30μL/h Nozzle-to-substrate distance: 2mm Substrate composition: Silicon Applied voltage: about 2kV x-y stage velocity: 1-20mm/s Fiber Diameter: 3.73 ± 1.37μm Distance between adjacent fibers: 5.13 ± 6.67μm
Poly(Vinylidene Fluoride) (PVDF; MW = 534,000 g/mol)	Acetone and Dimethyl Sulfoxide (DMSO)	3D Electrospinning	Solution Concentration: 17wt% PVDF; 1.7g of PVDF, 5g of acetone, 0.5g of Capstone FS-66, 5g of DMSO [26] Nozzle: Needle inner diameter of 100μm Solution deposition rate: 14 nL/min Nozzle-to-substrate distance: 750μm Substrate composition: A4 size commercial printing paper (Double A) Applied voltage: 1.9kV x-y stage velocity: 10mm/s Fiber Diameter: Not determined Distance between adjacent fibers: Not determined
Poly(9-Vinyl Carbazole) (PVK; MW = 1,100,000 g/mol)	Styrene	Typical NFES process	Solution Concentration: 3.96wt% PVK in styrene [25] Nozzle: Needle inner diameter of 100μm Solution deposition rate: 500nL/min Nozzle-to-substrate distance: around 2.5mm Substrate composition: Si/SiO ₂ Applied voltage: 3-4kV x-y stage velocity: 13.3cm/s Fiber Diameter: 289.26 ± 35.37nm Distance between adjacent fibers: 50μm Notes: 15m yield in 2min

Continued on next page

<i>Table 2 continued</i>				
Polystyrene (PS; MW <i>Not determined</i>)	1,2,4-Trichloro benzene	Electrohydrodynamic (EHD) jet printing	Solution Concentration: 1 to 5wt% PS Nozzle: Glass nozzle inner diameter of $2\mu m$ and outer diameter of $2.66\mu m$ Solution deposition rate: <i>Not determined</i> Nozzle-to-substrate distance: 20, 30, $40\mu m$ Substrate composition: Si Applied voltage: 500 to 400V in 25V increments x-y stage velocity: 0.01-10mm/s Fiber Diameter: about 60-170 μm Distance between adjacent fibers: <i>Not determined</i>	[23]
Poly(ethylene oxide) (PEO; MW = 300,000 g/mol)	<i>Not determined</i>	Typical NFES process	Solution Concentration: 3wt% PEO Nozzle: <i>Not determined</i> Solution deposition rate: <i>Not determined</i> Nozzle-to-substrate distance: 500 μm Substrate composition: Si Applied voltage: 1000V x-y stage velocity: 20cm/s Fiber Diameter: 300nm Distance between adjacent fibers: 25 μm	[16]
Poly(ethylene oxide) (PEO; MW = 2,000,000 g/mol)	Distilled water	Multinozzle NFES	Solution Concentration: 5wt% Nozzle: four-nozzle and six-nozzle array with needle spacing changes from 1.5mm to 3.5mm Solution deposition rate: 1-3 $\mu L/min$ Nozzle-to-substrate distance: 2mm Substrate composition: <i>Not determined</i> Applied voltage: 1.7-2.7kV x-y stage velocity: <i>Not determined</i> Fiber Diameter: 5.47 μm Distance between adjacent fibers: 3-5 mm	[33]

Continued on next page

Table 2 continued

Poly(ethylene oxide) (PEO; MW = 2,000,000 g/mol)	Distilled water	Multinozzle NFES	Solution Concentration: 5wt% Nozzle: Dual-28G-needle array with needle inner diameter of 0.18mm and outer diameter of 0.36mm; with needle spacing changes from 2.0mm to 3.0mm Solution deposition rate: 0.2μL/min Nozzle-to-substrate distance: 3.0-4.0mm Substrate composition: Not determined Applied voltage: 2.0-3.0kV x-y stage velocity: 20mm/s Fiber Diameter: Not determined Distance between adjacent fibers: 218-326μm	[34]
Poly(ethylene oxide) (PEO; MW = 2,000,000 g/mol)	Distilled water	Multinozzle NFES	Solution Concentration: 5 wt% Nozzle: Dual-28G-needle array with needle inner diameter of 180μm and outer diameter of 360μm; with needle spacing changes of 2.0mm Solution deposition rate: 0.2μL/min Nozzle-to-substrate distance: 4.0mm Substrate composition: chromium-plated glass Applied voltage: 2.5kV x-y stage velocity: 20mm/s Fiber Diameter: Not determined Distance between adjacent fibers: 2.3002-2.7224mm	[35]
Poly(ethylene oxide) (PEO; MW = 4,000,000 g/mol)	Not determined	Typical NFES process	Solution Concentration: 2wt% Nozzle: G30 needle with inner diameter of 0.15mm Solution deposition rate: Not determined Nozzle-to-substrate distance: 1-3mm Substrate composition: Silicon Applied voltage: 1250V x-y stage velocity: Not determined Fiber Diameter: Not determined Distance between adjacent fibers: 20μm	[27]

Continued on next page

Table 2 continued

Gelatin (porcine skin; MW <i>Not determined</i>)	Acetic Acid and Ethyl Acetate	Typical NFES pro- cess	Solution Concentration: 11wt% gelatin, 30wt% water, [18] 35.4wt% acetic acid, 23.6wt% ethyl acetate Nozzle: 19G needle tip with outer diameter of 1.08mm Solution deposition rate: <i>Not determined</i> Nozzle-to-substrate distance: 1.25mm Substrate composition: Poly(Dimethylsiloxane) (PDMS) films Applied voltage: 1000V x-y stage velocity: <i>Not determined</i> Fiber Diameter: around 2-3 μ m Distance between adjacent fibers: 40 μ m
Poly(ethylene ox- ide) (PEO; MW = 300,000 g/mol)	Water/Ethanol (v/v = 60/40)	Typical NFES pro- cess	Solution Concentration: PEO concentrations of 16% and [36] 18% Nozzle: 40 μ m Solution deposition rate: <i>Not determined</i> Nozzle-to-substrate distance: 1mm Substrate composition: Planar silicon Applied voltage: 1.7kV x-y stage velocity: 0.36m/s Fiber Diameter: 5.15 μ m Distance between adjacent fibers: <i>Not determined</i>
Poly(ethylene ox- ide) (PEO; MW = 300,000 g/mol)	Water/Ethanol (v/v = 3/1)	Electrohydro- dynamic Direct- Write (EDW)	Solution Concentration: 14wt% PEO [37] Nozzle: Stainless needle with inner diameter of 210 μ m and outer diameter of 400 μ m Solution deposition rate: 50 μ L/h Nozzle-to-substrate distance: 2mm Substrate composition: Poly(ethylene terephthalate) (PET) Applied voltage: 3kV x-y stage velocity: 700mm/s Fiber Diameter: 15-35 μ m Distance between adjacent fibers: 70 μ m

Continued on next page

Table 2 continued

Poly(ethylene oxide) (PEO; MW = 300,000 g/mol)	Deionized water	Mechano-Electrospinning		<p>Solution Concentration: 3wt% PEO [38]</p> <p>Nozzle: Stainless steel nozzle with inner diameter of 160μm and outer diameter of 310μm</p> <p>Solution deposition rate: 50nL/min</p> <p>Nozzle-to-substrate distance: 2-5mm</p> <p>Substrate composition: Silicone</p> <p>Applied voltage: polymer jet initiated at 2kV and dispensed at 1kV</p> <p>x-y stage velocity: 200-400mm/s</p> <p>Fiber Diameter: from 344\pm32 to 214\pm27nm</p> <p>Distance between adjacent fibers: Not determined</p>
Poly(co-Glycolic acid (PLGA; MW Not determined)	Dimethyl Carbonate (DMC)	Tethered Electrohydrodynamic (TPES)	Pyro-Spinning	<p>Solution Concentration: Not determined [19]</p> <p>Nozzle: nozzle-free</p> <p>Solution deposition rate: The drop reservoir is placed directly on a flat substrate</p> <p>Nozzle-to-substrate distance: Taylor's cone is focused and put in direct contact with the collector</p> <p>Substrate composition: Poly(tetrafluoroethylene) (PTFE) coated glass slide</p> <p>Applied voltage: pyro-electric field of between 2.7 $\times 10^7$ V/m and 5.5 $\times 10^7$ V/m</p> <p>x-y stage velocity: Not determined</p> <p>Fiber Diameter: 304.7nm</p> <p>Distance between adjacent fibers: Not determined</p>

Continued on next page

Table 2 continued

Poly(ethylene oxide) (PEO; MW = 4,000,000 g/mol) with Tetra-butylammonium tetrafluoroborate (TBF; MW Not determined) and SU-8 2002	N,N Dimethyl-formamide (DMF)	Typical NFES process	Solution Concentration: SU-8/PEO/TBF blend with 0.75wt% PEO, 1wt% TBF; the blend is diluted with 30vol% DMF $\mu m \mu m$ Solution deposition rate: <i>Not determined</i> Nozzle-to-substrate distance: <i>Not determined</i> Substrate composition: Brass disk with a diameter of 38mm Applied voltage: 980V x-y stage velocity: <i>Not determined</i> Fiber Diameter: <i>Not determined</i> Distance between adjacent fibers: <i>Not determined</i>	[6]
Poly(ethylene oxide) (PEO; 200,000 g/mol)	Water:Ethanol (3:2)	Suspension NFES	Solution Concentration: 14wt% PEO Nozzle: stainless steel needle (25 G) with inner diameter of 0.25mm Solution deposition rate: 3nL/s Nozzle-to-substrate distance: between 0.5 and 10mm with 0.5mm increments Substrate composition: Planar silicon electrodes Applied voltage: 1.6kV x-y stage velocity: 50, 150, and 250mm/s Fiber Diameter: 300nm Distance between adjacent fibers: 0.1 and 0.5mm	[39]
Poly(ethylene oxide) (PEO; MW = 400,000 g/mol)	Deionized water	Typical NFES process	Solution Concentration: 10wt% PEO Nozzle: 32G metal needle Solution deposition rate: (Jet impact speed of 5mm/s) Nozzle-to-substrate distance: 0.5mm Substrate composition: p-type silicon wafer Applied voltage: 400V x-y stage velocity: 5mm/s Fiber Diameter: <i>Not determined</i> Distance between adjacent fibers: 50 μm	[40]

5. NFES Variants

[SECTION to be REMOVED]

Nanofibers are fibers with diameters in the nanometer range. The development of nanofibers has greatly enhanced the scope for meeting up the modern world challenges.

Currently there are two types of electrospinning systems available for producing nanofiber: needle based electrospinning and needleless electrospinning. This paper summarizes the basic mechanism of various types of needle based and needleless spinning systems described in various literatures by many researchers.

5.1. Low-Voltage NFES (LV NFES) [8]

Some differences have been discovered between LV-NFES and conventional NFES. Low voltage near field electrospinning produces thinner fibers with lower voltages. Moreover, when implementing a moving stage, the fibers are affected by the mechanical stretching. Bisht et al. [8] reported that thinner diameters are yield with the increase of the x-y stage velocity, and larger diameters by decreasing the stage velocity.

5.2. Scanning Tip Electrospinning [9]

Lorem ipsum dolor sit amet, consectetur adipiscing elit, sed do eiusmod tempor incididunt ut labore et dolore magna aliqua.

5.3. 3D Electrospinning [26]

Electrohydro-dynamic 3D Print-patterning or Electrohydro-dynamic Jetting [17]

Lorem ipsum dolor sit amet, consectetur adipiscing elit, sed do eiusmod tempor incididunt ut labore et dolore magna aliqua.

5.4. Multinozzle NFES [33–35]

Lorem ipsum dolor sit amet, consectetur adipiscing elit, sed do eiusmod tempor incididunt ut labore et dolore magna aliqua.

5.5. Electrohydro-dynamic Writing or Mechano-electrospinning (MES) [24]

Electrohydro-dynamic Direct-Write (EDW) [37]

Mechano-Electrospinning [38]

Lorem ipsum dolor sit amet, consectetur adipiscing elit, sed do eiusmod tempor incididunt ut labore et dolore magna aliqua.

5.6. Suspension NFES [39]

Lorem ipsum dolor sit amet, consectetur adipiscing elit, sed do eiusmod tempor incididunt ut labore et dolore magna aliqua.

5.7. Helix Electrohydro-dynamic Printing (HE-printing) [31]

Electrohydro-dynamic (EHD) jet printing [23]

Lorem ipsum dolor sit amet, consectetur adipiscing elit, sed do eiusmod tempor incididunt ut labore et dolore magna aliqua.

5.8. Airflow-assisted Electrohydro-dynamic Direct-writing (EDW) [32]

Lorem ipsum dolor sit amet, consectetur adipiscing elit, sed do eiusmod tempor incididunt ut labore et dolore magna aliqua.

5.9. Tethered Pyro-Electrohydro-dynamic Spinning (TPES) [19]

Lorem ipsum dolor sit amet, consectetur adipiscing elit, sed do eiusmod tempor incididunt ut labore et dolore magna aliqua.

6. Conclusion

Lorem ipsum dolor sit amet, consectetur adipiscing elit, sed do eiusmod tempor incididunt ut labore et dolore magna aliqua. Ut enim ad minim veniam, quis nostrud exercitation ullamco laboris nisi ut aliquip ex ea commodo consequat. Duis aute irure dolor in reprehenderit in voluptate velit esse cillum dolore eu fugiat nulla pariatur. Excepteur sint occaecat cupidatat non proident, sunt in culpa qui officia deserunt mollit anim id est laborum.

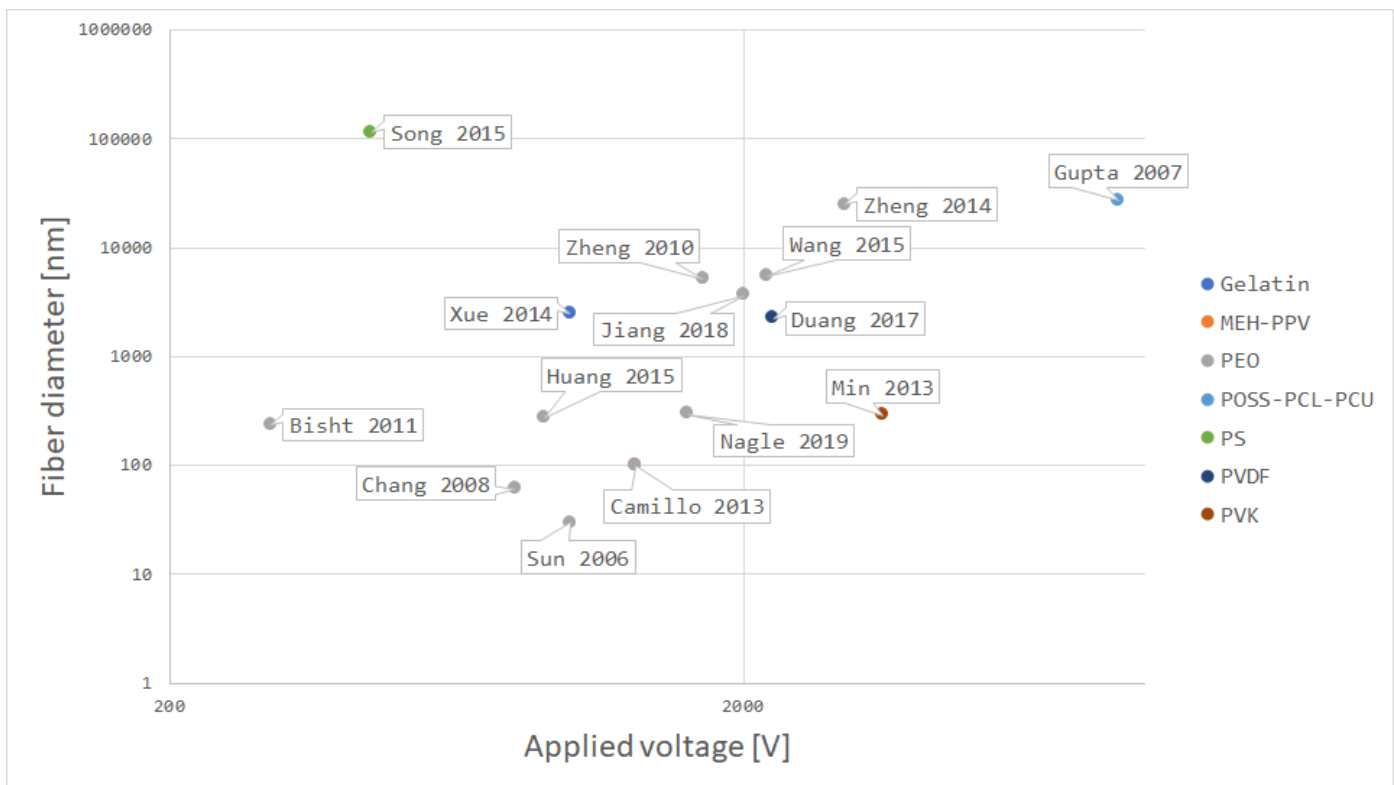


Figure 4: Applied volage vs. Fiber diameter

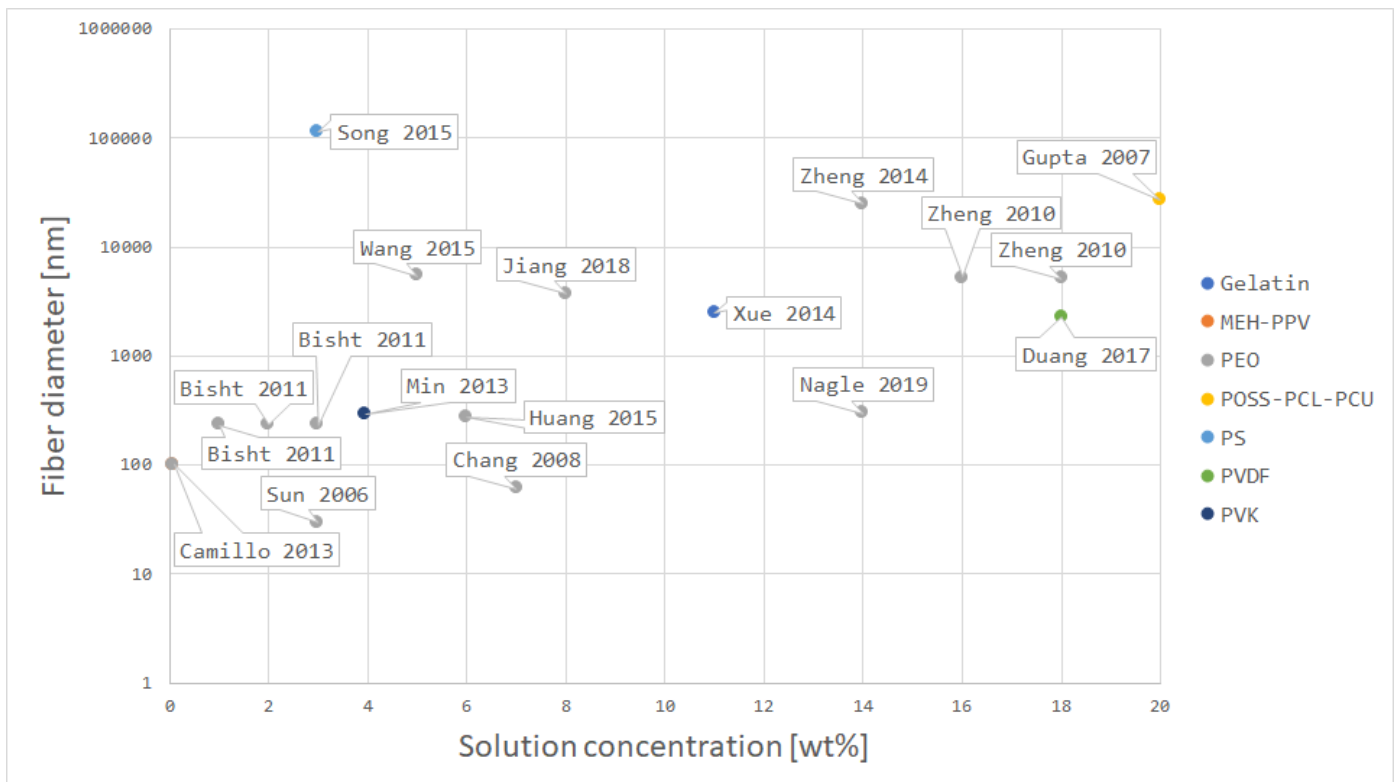


Figure 5: Solution concentration vs. Fiber diameter

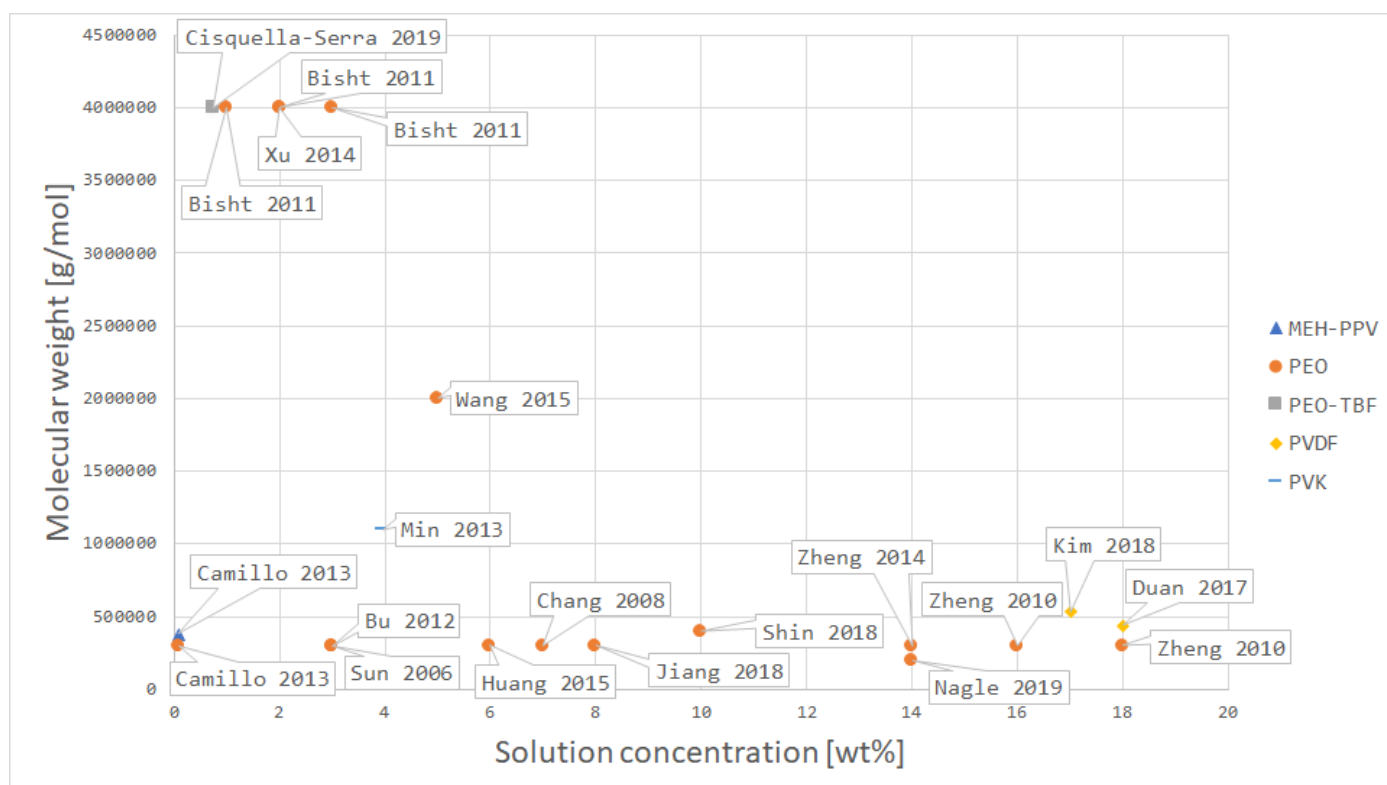


Figure 6: Solution concentration vs. Molecular weight

7. NFES Achievements & Challenges

Lorem ipsum dolor sit amet, consectetur adipiscing elit, sed do eiusmod tempor incididunt ut labore et dolore magna aliqua. Ut enim ad minim veniam, quis nostrud exercitation ullamco laboris nisi ut aliquip ex ea commodo consequat. Duis aute irure dolor in reprehenderit in voluptate velit esse cillum dolore eu fugiat nulla pariatur. Excepteur sint occaecat cupidatat non proident, sunt in culpa qui officia deserunt mollit anim id est laborum.

References

- [1] F. Anton, Process and apparatus for preparing artificial threads (1930). doi:<https://patents.google.com/?q=D01D5%2f0076>.
- [2] Z.-M. Huang, Y. Z. Zhang, M. Kotaki, S. Ramakrishna, A review on polymer nanofibers by electrospinning and their applications in nanocomposites, *Composites Science and Technology* 63 (15) (2003) 2223–2253. doi:10.1016/S0266-3538(03)00178-7.
- [3] D. H. Reneker, A. L. Yarin, Electrospinning jets and polymer nanofibers, *Polymer* 49 (10) (2008) 2387–2425. doi:10.1016/J.POLYMER.2008.02.002.
- [4] J. D. Schiffman, C. L. Schauer, A Review: Electrospinning of Biopolymer Nanofibers and their Applications, *Polymer Reviews* 48 (2) (2008) 317–352. doi:10.1080/15583720802022182.
- [5] Q. Li, Chapter 7: Liquid Crystal-Functionalized Nano- and Microfibers Produced by Electrospinning - Liquid Crystals Beyond Displays: Chemistry, Physics, and Applications, John Wiley & Sons, 2012. doi:9781118078617.
- [6] A. Cisquella-Serra, M. Magnani, Álvaro Gual-Mosegui, S. Holmberg, M. Madou, M. Gamero-Castaño, Study of the electrostatic jet initiation in near-field electrospinning, *Journal of Colloid and Interface Science* 543 (2019) 106–113. doi:10.1016/J.JCIS.2019.02.041.
- [7] S. K. Nataraj, K. S. Yang, T. M. Aminabhavi, Polyacrylonitrile-based nanofibers—A state-of-the-art review, *Progress in Polymer Science* 37 (3) (2012) 487–513. doi:10.1016/J.PROGPOLYMSCI.2011.07.001.
- [8] G. S. Bisht, G. Canton, A. Mirsepassi, L. Kulinsky, S. Oh, D. Dunn-Rankin, M. J. Madou, Controlled Continuous Patterning of Polymeric Nanofibers on Three-Dimensional Substrates Using Low-Voltage Near-Field Electrospinning, *Nano Letters* 11 (4) (2011) 1831–1837. doi:10.1021/nl2006164.
- [9] C. Chang, K. Limkraisassiri, L. Lin, Continuous near-field electrospinning for large area deposition of

- orderly nanofiber patterns, *Appl Phys Lett* (2008) 3doi:10.1063/1.2975834.
- [10] J. Zheng, Y. Z. Long, B. Sun, Z. H. Zhang, F. Shao, H. D. Zhang, Z. M. Zhang, J. Y. Huang, Polymer nanofibers prepared by low-voltage near-field electrospinning, *Chinese Physics B* 21 (4) (2012) 1–6. doi:10.1088/1674-1056/21/4/048102.
 - [11] C.-T. Pan, C.-K. Yen, Z.-H. Liu, H.-W. Li, S.-W. Kuo, Y.-S. Lu, Y.-C. Lai, Poly(γ -benzyl α -l-glutamate) in Cylindrical Near-Field Electrospinning Fabrication and Analysis of Piezoelectric Fibers (2014).
 - [12] C.-T. Pan, C.-K. Yen, S.-Y. Wang, Y.-C. Lai, L. Lin, J. C. Huang, S.-W. Kuo, Near-field electrospinning enhances the energy harvesting of hollow PVDF piezoelectric fibers, *RSC Advances* 5 (103) (2015) 85073–85081. doi:10.1039/C5RA16604G.
 - [13] S. Chakraborty, I.-C. Liao, A. Adler, K. W. Leong, Electrohydrodynamics: A facile technique to fabricate drug delivery systems, *Advanced Drug Delivery Reviews* 61 (12) (2009) 1043–1054. doi:10.1016/j.addr.2009.07.013.
 - [14] K. A. G. Katsogiannis, G. T. Vladislavljević, S. Georgiadou, Porous electrospun polycaprolactone (PCL) fibres by phase separation, *European Polymer Journal* 69 (2015) 284–295. doi:10.1016/j.eurpolymj.2015.01.028.
 - [15] J. Kameoka, H. G. Craighead, Fabrication of oriented polymeric nanofibers on planar surfaces by electrospinning, *Applied Physics Letters* 83 (2) (2003) 371–373. doi:10.1063/1.1592638.
 - [16] D. Sun, C. Chang, S. Li, L. Lin, Near-Field Electrospinning (2006). doi:10.1021/nl0602701.
 - [17] A. Gupta, A. M. Seifalian, Z. Ahmad, M. J. Edirisinghe, M. C. Winslet, Novel Electrohydrodynamic Printing of Nanocomposite Biopolymer Scaffolds, *Journal of BIOACTIVE AND COMPATIBLE POLYMERS* 22 (2007). doi:10.1177/0883911507078268.
 - [18] N. Xue, X. Li, C. Bertulli, Z. Li, A. Patharagulpong, A. Sadok, Y. Y. S. Huang, Rapid Patterning of 1-D Collagenous Topography as an ECM Protein Fibril Platform for Image Cytometry, *PLoS ONE* 9 (4) (2014) e93590. doi:10.1371/journal.pone.0093590.
 - [19] S. Coppola, V. Vespini, G. Nasti, O. Gennari, S. Grilli, M. Ventre, M. Iannone, P. A. Netti, P. Ferraro, Tethered Pyro-Electrohydrodynamic Spinning for Patterning Well-Ordered Structures at Micro- and Nanoscale, *Chem. Mater* 26 (2014) 3360. doi:10.1021/cm501265j.
 - [20] D. D. Camillo, V. Fasano, F. Ruggieri, S. Santucci, L. Lozzi, A. Camposeo, D. Pisignano, Near-field electrospinning of conjugated polymer light-emitting nanofibers, *Nanoscale* 5 (2013) 11637–11642. doi:10.1039/C3NR03094F.
 - [21] Q. Xiang, Y.-M. Ma, D.-G. Yu, M. Jin, G. R. Williams, Electrospinning using a Teflon-coated spinneret, *Applied Surface Science* 284 (2013) 889–893. doi:10.1016/j.apsusc.2013.08.030.
 - [22] Q. Wang, D. G. Yu, S. Y. Zhou, C. Li, M. Zhao, Electrospun amorphous medicated nanocomposites fabricated using a Teflon-based concentric spinneret, *E-Polymers* 18 (1) (2018) 3–11. doi:10.1515/epoly-2017-0110.
 - [23] C. Song, J. A. Rogers, J.-M. Kim, H. Ahn, Patterned polydiacetylene-embedded polystyrene nanofibers based on electrohydrodynamic jet printing, *Macromolecular Research* 23 (1) (2015) 118–123. doi:10.1007/s13233-015-3024-2.
 - [24] Y. Huang, Y. Duan, Y. Ding, N. Bu, Y. Pan, N. Lu, Z. Yin, Versatile, kinetically controlled, high precision electrohydrodynamic writing of micro/nanofibers, *Scientific Reports* 4 (1) (2015) 5949. doi:10.1038/srep05949.
 - [25] S.-Y. Min, T.-S. Kim, B. J. Kim, H. Cho, Y.-Y. Noh, H. Yang, J. H. Cho, T.-W. Lee, Large-scale organic nanowire lithography and electronics, *Nature Communications* 4 (1) (2013) 1773. doi:10.1038/ncomms2785.
 - [26] J. Kim, B. Maeng, J. Park, Characterization of 3D electrospinning on inkjet printed conductive pattern on paper, *Micro and Nano Systems Letters* 6 (1) (2018) 12. doi:10.1186/s40486-018-0074-1.
 - [27] J. Xu, M. Abecassis, Z. Zhang, P. Guo, J. Huang, K. Ehmann, J. Cao, Accuracy Improvement of Nano-fiber Deposition by Near-Field Electrospinning, *International Workshop on Microfactories IWFMF2014 (9th)* (2014).
 - [28] Z. H. Liu, C. T. Pan, L. W. Lin, J. C. Huang, Z. Y. Ou, Direct-write PVDF nonwoven fiber fabric energy harvesters via the hollow cylindrical near-field electrospinning process (2014) 25003–25014doi:10.1088/0964-1726/23/2/025003.
 - [29] W. S. Choi, G. H. Kim, J. H. Shin, G. Lim, T. An, Electrospinning onto Insulating Substrates by Controlling Surface Wettability and Humidity, *Nanoscale Research Letters* 12 (2017). doi:10.1186/s11671-017-2380-6.
 - [30] D. D. Camillo, V. Fasano, F. Ruggieri, S. Santucci, L. Lozzi, A. Camposeo, D. Pisignano, Near-field electrospinning of conjugated polymer light-emitting nanofibers, *Nanoscale* 5 (2013) 11637–11642. doi:10.1039/C3NR03094F.
 - [31] Y. Duan, Y. Ding, Z. Xu, Y. Huang, Z. Yin, Helix Electrohydrodynamic Printing of Highly Aligned Serpentine Micro/Nanofibers., *Polymers* 9 (9) (sep 2017). doi:10.3390/polym9090434.
 - [32] J. Jiang, X. Wang, W. Li, J. Liu, Y. Liu, G. Zheng, J. Jiang, X. Wang, W. Li, J. Liu, Y. Liu, G. Zheng, Electrohydrodynamic Direct-Writing Micropatterns with Assisted Airflow, *Micromachines* 9 (9) (2018) 456. doi:10.3390/mi9090456.

- [33] H. Wang, S. Huang, F. Liang, P. Wu, M. Li, S. Lin, X. Chen, Research on Multinozzle Near-Field Electrospinning Patterned Deposition, *Journal of Nanomaterials* 2015 (2015) 1–8. doi:10.1155/2015/529138.
- [34] Z. Wang, X. Chen, J. Zeng, F. Liang, P. Wu, H. Wang, Controllable deposition distance of aligned pattern via dual-nozzle near-field electrospinning, *AIP Advances* 7 (3) (2017) 035310. doi:10.1063/1.4974936.
- [35] Z. Wang, X. Chen, J. Zhang, Y.-J. Lin, K. Li, J. Zeng, P. Wu, Y. He, Y. Li, H. Wang, Fabrication and evaluation of controllable deposition distance for aligned pattern by multi-nozzle near-field electrospinning, *AIP Advances* 8 (7) (2018) 075111. doi:10.1063/1.5032082.
- [36] G. Zheng, W. Li, X. Wang, D. Wu, D. Sun, L. Lin, Precision deposition of a nanofibre by near-field electrospinning, *Journal of Physics D: Applied Physics* 43 (41) (2010) 415501. doi:10.1088/0022-3727/43/41/415501.
- [37] J.-Y. Zheng, H.-Y. Liu, X. Wang, Y. Zhao, W.-W. Huang, G.-F. Zheng, D.-H. Sun, Electrohydrodynamic Direct-Write Orderly Micro/Nanofibrous Structure on Flexible Insulating Substrate, *Journal of Nanomaterials* 2014 (2014) 1–7. doi:10.1155/2014/708186.
- [38] N. Bu, Y. Huang, X. Wang, Z. Yin, Materials and Manufacturing Processes Continuously Tunable and Oriented Nanofiber Direct-Written by Mechano-Electrospinning Continuously Tunable and Oriented Nanofiber Direct-Written by Mechano-Electrospinning (2012). doi:10.1080/10426914.2012.700145.
- [39] A. R. Nagle, C. D. Fay, Z. Xie, G. G. Wallace, X. Wang, M. J. Higgins, A direct 3D suspension near-field electrospinning technique for the fabrication of polymer nanoarrays, *Nanotechnology* 30 (19) (2019) 195301. doi:10.1088/1361-6528/ab011b.
- [40] D. Shin, J. Kim, J. Chang, Experimental study on jet impact speed in near-field electrospinning for precise patterning of nanofiber, *Journal of Manufacturing Processes* 36 (2018) 231–237. doi:10.1016/J.JMAPRO.2018.10.011.